Chinese Herbal Medicines 15 (2023) 139–150

Contents lists available at ScienceDirect

Chinese Herbal Medicines

journal homepage: www.elsevier.com/locate/chmed

Original Article

Identification of prototype compounds and their metabolites in rats' serum from Xuefu Zhuyu Decoction by UPLC-Q-TOF/MS

Xiaoyu Zhang [a,1], Zhenzuo Jiang [a,1], Lei Zhang [a,1], Cheng Xue [a], Xiafei Feng [b], Xin Chai [a], Yuefei Wang [a,*]

[a] State Key Laboratory of Component-based Chinese Medicine, Tianjin Key Laboratory of TCM Chemistry and Analysis, Tianjin University of Traditional Chinese Medicine, Tianjin 301617, China
[b] Foreign Language College, Donghua University, Shanghai 201620, China

ARTICLE INFO

Article history:
Received 5 January 2022
Revised 13 April 2022
Accepted 10 August 2022
Available online 20 September 2022

Keywords:
metabolites
prototype compounds
serum
UPLC-Q-TOF/MS
Xuefu Zhuyu Decoction

ABSTRACT

Objective: As a classic prescription in traditional Chinese medicine, Xuefu Zhuyu Decoction (XFZYD) has been widely used in the clinical treatment of cardiovascular and cerebrovascular diseases. In order to unveil the potentially effective compounds, a rapid ultra-performance liquid chromatography coupled with quadrupole time-of-flight mass spectrometry (UPLC-Q-TOF/MS) method was established to identify prototype compounds and their metabolites from XFZYD in rats' serum.

Methods: The serum from rats after intragastric administration of XFZYD aqueous extract was analyzed by UPLC-Q-TOF/MS method. The prototype compounds and their metabolites were identified by comparison with the reference standards and tentatively characterized by comprehensively analyzing the retention time, MS data, characteristic MS fragmentation pattern and retrieving literatures.

Results: A total of 175 compounds (24 prototype compounds and 151 metabolites) were identified and tentatively characterized. The metabolic pathways of prototype compounds *in vivo* were also summarized, including glucuronidation, hydrolyzation, sulfation, demethylation, and hydroxylation, and so on.

Conclusion: In this study, a UPLC-Q-TOF/MS technique was developed to analyze prototype compounds and their metabolites from XFZYD in serum, which would provide the evidence for further studying the effective compounds of XFZYD.

1. Introduction

Xuefu Zhuyu Decoction (XFZYD), developed by Qingren Wang (1768–1831) in *Yilin Gaicuo* (Correction of Medical Errors, 1850), is a well-known traditional Chinese medicine formula. XFZYD consists of eleven herbs, including *Persicae Semen* (Taoren), *Angelicae Sinensis Radix* (Danggui), *Chuanxiong Rhizoma* (Chuanxiong), *Carthami Flos* (Honghua), *Paeoniae Radix Rubra* (Chishao), *Rehmanniae Radix* (Dihuang), *Aurantii Fructus* (Zhiqiao), *Bupleuri Radix* (Chaihu), *Platycodonis Radix* (Jiegeng), *Achyranthis Bidentatae Radix* (Niuxi), and *Glycyrrhizae Radix* et *Rhizoma* (Gancao), which is widely used to treat diseases caused by *qi* stagnation and blood stasis with its effects of blood-activating, stasis-resolving and regulating *qi*-flowing (Wang, 2005; Wang et al., 2022). It was reported that XFZYD has the significant clinical effects on dysmenorrhoea, traumatic brain injury, and endometriosis (Jo et al., 2017; Zhang & Yuan et al., 2018; Fu et al., 2019; Su, Zeng & Zeng, 2020). Especially, XFZYD is widely employed to treat cardiovascular diseases, including chest pain, headache, angina pectoris, heart failure, atherosclerosis, hypertension, and hyperlipidemia as the basic prescription (Yang et al., 2019; Lin et al., 2018; Jiang & Jiang, 2016; Wang, Xiong, & Li, 2015; Wang & Qiu, 2019; Meng et al., 2018). However, its underlying action mechanism is still uncovered. Importantly, the clarification of chemical compounds *in vivo* is the prerequisite question which must be answered and worthy of in-depth study.

In recent years, researchers have made continuous efforts to develop various analytical methods to clarify the chemical compounds of XFZYD. Previously, our group employed ultra performance liquid chromatography with diode array detector tandem mass spectrometry (UPLC-DAD-MS/MS) method to identify 28 compounds and quantitatively analyze 12 compounds in XFZYD related products (Zhang et al., 2012). Also, we made use of ultra performance liquid chromatography coupled with quadrupole time-of-flight mass spectrometry (UPLC-Q-TOF/MS) to systematically illuminate the chemical compounds of XFZYD *in vitro*, by which 103 compounds were identified, mainly including phenolic acids, flavonoids, saponins, terpenes, and other compounds

* Corresponding author.
E-mail address: wangyf0622@tjutcm.edu.cn (Y. Wang).
[1] These authors contributed equally to this work.

https://doi.org/10.1016/j.chmed.2022.08.002
1674-6384/

(Zhang et al., 2015). Besides this, Fu et al (2016) qualitatively analyzed 34 major constituents, including organic acids, lactones, alkaloids, amino acids and cyanogenic glycosides in XFZYD by using ultra high performance liquid chromatography with hybrid ion trap time-of-flight mass spectrometry (UHPLC-ESI-IT-TOF-MS). However, there are few reports on clarification of the prototype compounds and their metabolites from XFZYD exposed *in vivo*, which will be important for illuminating the potentially active compounds. The metabolites always act as the active compounds *in vivo*. For instance, dihydroberberine, jatrorrhizine, columbamine, berberrubine, and demethyleneberberine, the metabolites of berberine produced by intestinal microbiota, have the significant effect of lipid-lowering (Feng et al., 2018; Zuo et al., 2006; Zhou et al., 2014). Therefore, it is essential to study the exposed compounds from XFZYD *in vivo*.

In this study, we employed UPLC-Q-TOF/MS for identification of chemical compounds and their metabolites in rats' serum after oral administration of XFZYD aqueous extract at a dose of 16.38 g/kg body weight, which was expressed as the weight of decoction pieces. A total of 175 compounds were characterized and tentatively identified, including 24 prototype compounds and 151 metabolites. Also, the major metabolic pathways of prototype compounds from XFZYD in serum have been preliminarily proposed. Meaningfully, we established an analytical method with high sensitivity, rapid analysis, low consumption of samples, and abundant yield of structural information. Our study not only provides the information about the chemical substances of XFZYD *in vivo*, but also highly contributes to further investigation of the pharmacology and mechanism of XFZYD.

2. Materials and methods

2.1. Chemicals and materials

Acetonitrile and methanol (HPLC grade) were purchased from Fisher Scientific (Fisher, USA). Formic acid and dimethyl sulfoxide were purchased from Meridian Medical Technologies (MREDA, USA). Water for UPLC analysis was purified by a Milli-Q water purification system (Millipore, USA). Reference compounds, including *p*-hydroxybenzoic acid (PHBA), hydroxysafflor yellow A (HSYA), amygdalin, *p*-hydroxycinnamic acid (PHCA), ferulic acid, albiflorin, paeoniflorin, liquiritin, isoquercitrin, narirutin, *β*-ecdysterone, naringin, rhoifolin, hesperidin, neohesperidin, liquiritigenin, naringenin, platycodin D, isoliquiritigenin, formononetin, ginsenoside-Ro, 18*β*-glycyrrhizic acid, nobiletin, and saikosaponin A were obtained from the National Institutes for Food and Drug Control (Beijing, China), Tianjin ZhongXin Pharmaceutical Group Co., Ltd. (Tianjin, China), and Top High Bio Technology Co., Ltd. (Nanjing, China). The purity of standards was above 98%. All samples were stored at 4 °C before analysis.

2.2. Preparation of standard solution

As individual standard stock solution, reference compounds were accurately weighed and directly prepared in methanol by using dimethyl sulfoxide as a cosolvent. Then, a mixed standard solution was prepared at about 5 μg/mL. All solution of reference standards was stored at 4 °C.

2.3. UPLC-Q-TOF/MS analytical conditions

2.3.1. Chromatographic conditions

Chromatographic analysis was performed on an ACQUITY™ UPLC system (Waters, Milford, USA) equipped with a binary solvent manager, sample manager and column oven, which was controlled by Masslynx V4.1 software. Chromatographic separation was carried out on an ACQUITY™ UPLC BEH C_{18} column (2.1 × 100 mm, 1.7 μm) held at 50 °C. The flow rate was set at 0.3 mL/min. The mobile phase consisted of 0.1% formic acid aqueous solution (A) and acetonitrile (B) in a gradient elution. The program applied was as follows: 0–6.5 min, 3%–11% B; 6.5–15 min, 11%–20% B; 15–20 min, 20%–36% B; 20–27 min, 36%–48% B; 27–30 min, 48%–55% B; 30–33 min, 55%–74% B, and 33–35 min, 74%–90%. The injection volume of the sample solution was 5 μL.

2.3.2. MS spectrometry conditions

The MS analysis was performed by employing a Waters ACQUITY SYNAPT™ G2-S high definition mass spectrometer system (Waters, Milford, USA) equipped with an electrospray ion (ESI) source. The optimal conditions were as follows: capillary voltage at 3.0 and −2.5 kV in positive and negative ion mode, respectively; sampling cone voltage at 40 V; source temperature at 120 °C; desolvation temperature at 400 °C; the flow rate of cone gas and desolvation gas (N_2) at 50 L/h and 700 L/h, respectively; the flow rate of collision gas (Ar) at 0.20 mL/min. Data were acquired in centroid mode from *m*/*z* 100 to 1500 Da. For accurate mass to charge ratio acquisition, the MS was corrected during data acquisition using a lock mass of leucine-enkephalin (LE) at a concentration of 200 pg/mL via a LockSpray™ interface at a flow rate of 10 μL/min, monitoring the reference ions in the positive ion mode ($[M+H]^+$ = 556.2771) and the negative ion mode ($[M-H]^-$ = 554.2615) during MS analysis.

2.4. Preparation of XFZYD

The decoction pieces (Taoren, Danggui, Chuanxiong, Honghua, Chishao, Dihuang, Zhiqiao, Chaihu, Jiegeng, Niuxi, and Gancao) were purchased from Anguo Oriental Medical Town (Hebei, China) and identified by Professor Tianxiang Li, which were deposited in Tianjin Key Laboratory of TCM Chemistry and Analysis (Tianjin, China).

According to the regulation of XFZYD, the decoction pieces (total weight of 78 g) were mixed and immersed in 600 mL deionized water for 1 h at room temperature, and then refluxed twice for two hours per time. After filtration and concentration, aqueous extract was dried at 45 °C in an oven under vacuum to give 30 g extract powder, the yield of which was 38.5%. The extract powder was stored at 4 °C before use.

2.5. Animals and drug administration

Male Sprague-Dawley (SD) rats (200 ± 10 g) were supplied by Beijing HFK Bioscience Co., Ltd. (SCXK2009-0004, Beijing, China). All animals were acclimated in a room (22–25 °C with 50% ± 10% humidity) for one week, which had free access to water and standard laboratory food, and gradually adapted to the facilities. Then, the rats were fasted with free access to water for 12 h prior to the experiment. For seven consecutive days, the aqueous extract of XFZYD was administrated to the rats intragastrically at a dose of 16.38 g/kg body weight, which was expressed as the weight of decoction pieces (Zhang & Kang et al., 2018; Fan et al., 2020). After the last administration, the blood samples were respectively collected from the retroorbital venous plexuses at 0.5, 1 and 2 h, which were placed at room temperature for 1 h and centrifuged at 8000 rpm for 10 min. Then, the serum samples were obtained from the different blood sampling time in one rat and equally mixed to acquire the blended serum samples, which were frozen immediately and stored at −80 °C until analysis. Blank serum samples were collected in the same way. Animal studies were conducted according to protocols approved by the Review Committee of Animal Care and Use.

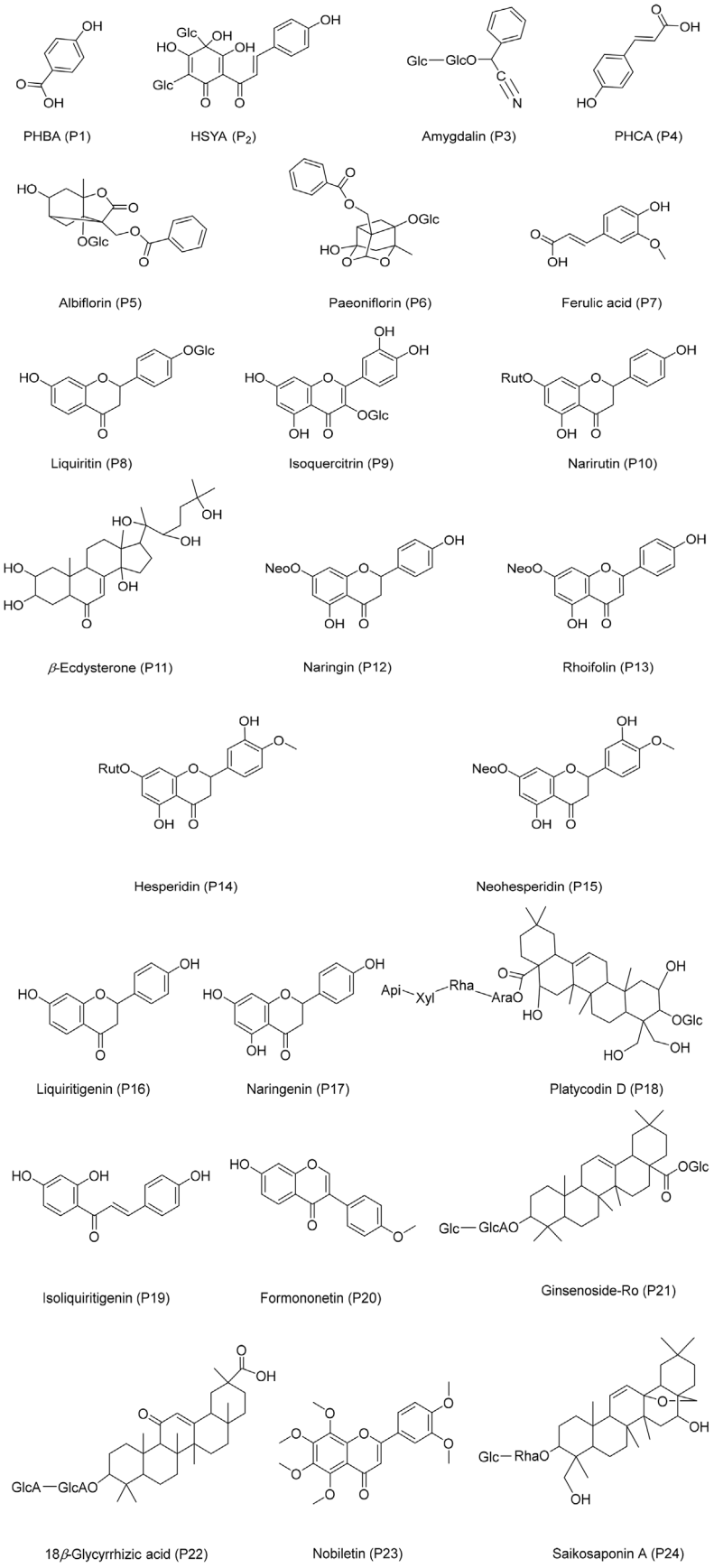

Fig. 1. Chemical structures of prototype compounds.

2.6. Sample preparation

The serum samples were thawed and homogenized at room temperature in advance. After addition of 10% formic acid (10 μL) in serum (1 mL), the sample was vortex-mixed well and loaded on Cleanert S C18-SPE column (500 mg/3 mL, Bonna-Agela, China), which was respectively pretreated with 2 mL methanol and 2 mL water, and equilibrated with 3 mL 1% formic acid in sequence. The loaded sample was sequently eluted with 3 mL 1% formic acid and 2 mL methanol, then methanol eluant was collected and evaporated to dryness by a vacuum centrifugal concentrator (Eppendorf, Hamburg, Germany) at 40 °C. Finally, the residue was dissolved in 50% methanol (100 μL) for analysis.

2.7. Statistical analysis

All the MS data were acquired and processed by Masslynx V4.1 software (Waters Corporation, Milford, MA, USA). The structures of prototype compounds were drawn using ChemBioDraw 14 software (CambridgeSoft Corporation, USA). The network was portrayed by Cytoscape V3.8.0 software (National Resource for Network Biology, USA).

3. Results and discussion

3.1. Optimization of pretreatment method and analytical condition

In order to remove interfering substances in serum samples and enrich the targeted compounds for more sensitive detection, serum samples were generally pretreated by the methods of protein precipitation, liquid–liquid extraction and solid-phase extraction, respectively (Feng et al., 2020; Yan et al., 2019; Zhang et al., 2019). Moreover, addition of a certain amount of acid, the performance of pretreatment can be improved for the acidic compounds. By our study, Cleanert S C18-SPE column (500 mg/3 mL, Bonna-Agela, China) was proved to be suitable as pretreatment method for the serum sample, resulting in the excellent enrichment of the interesting compounds and the satisfactory elimination of interfering signal in MS analysis. The structures of the detected prototype compounds are displayed in Fig. 1.

Furthermore, chromatographic separation and MS detection were accomplished to excellently detect the interesting compounds. Acetonitrile – water as the mobile phase system was optimized through adding 0.1% formic acid in water by taking the characteristics of acidic and alkaline analytes into account. Aiming

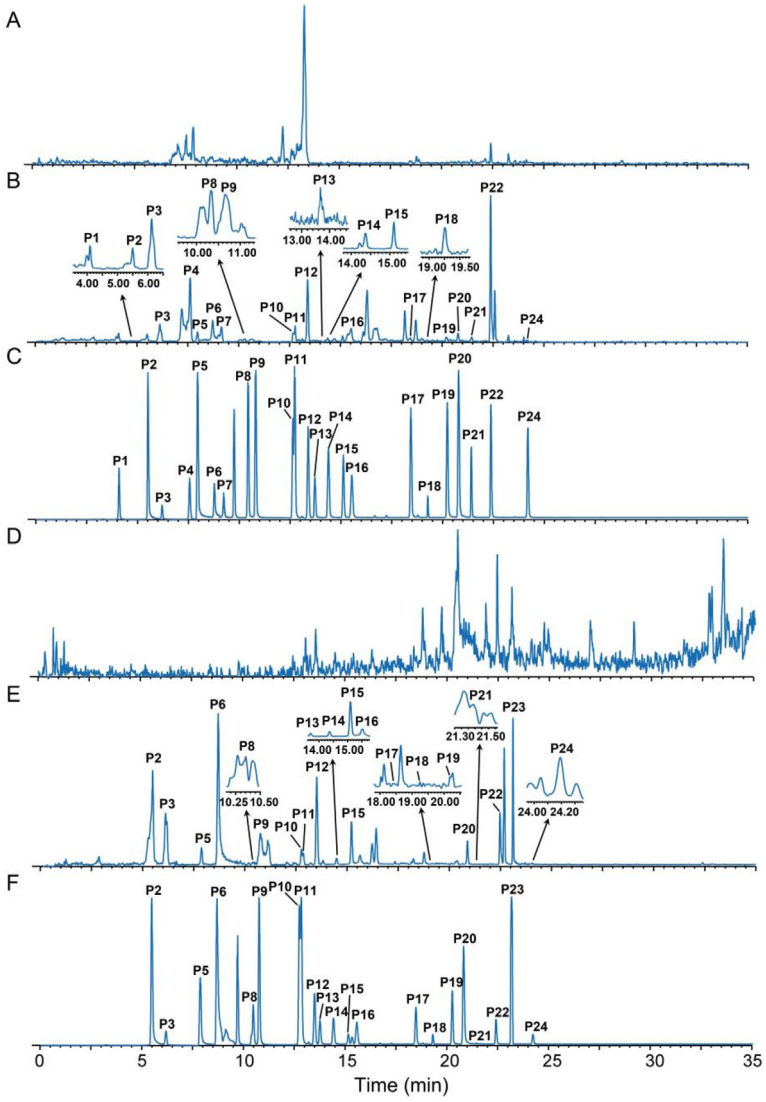

Fig. 2. Extracted ion chromatograms of prototype compounds from serum sample solution and mixed standards solution (Blank serum sample (A), dosed serum sample (B), and mixed standards sample (C) in negative mode; Blank serum sample (D), dosed serum sample (E), and mixed standards sample (F) in positive mode.

at obtaining comprehensive MS information of analytes as much as possible, UPLC-Q-TOF/MS was performed in positive and negative ion modes. Because of the existence of phenolic hydroxyl and carboxyl groups in the analytes, it is found that the negative ion mode has good MS response.

3.2. Identification of prototype compounds from XFZYD in serum

Illumination of prototype compounds absorbed into blood is the prerequisite issue to clarify the exposure of chemical compounds *in vivo* from Chinese materia medica (CMM), which will pave the way for identification of metabolites derived from these prototype compounds. Through our previous study, flavanones, saponins and phenolic acids were proven to be the representative compounds in XFZYD (Zhang et al., 2012; Zhang et al., 2015). In our study, characterization of prototype compounds was performed from the dosed serum by analyzing the blank serum, dosed serum, and reference standards. The extracted ion chromatograms of prototype compounds from the serum samples and mixed standards are shown in Fig. 2. Compared the MS data of the serum samples with those of authentic compounds (Table 1 and Supplementary Table S1), 24 prototype compounds were characterized, including 13 flavanones (HSYA, liquiritin, isoquercitrin, narirutin, naringin, rhoifolin, hesperidin, neohesperidin, liquiritigenin, naringenin, isoliquiritigenin, formononetin and nobiletin), four saponins (platycodin D, ginsenoside-Ro, 18β-glycyrrhizic acid and saikosaponin A), three phenolic acids (PHBA, PHCA, and ferulic acid), and four others (β-ecdysterone, amygdalin, albiflorin and paeoniflorin).

Studies have shown that the prototype compounds identified in XFZYD play an important role in the prevention and treatment of cardiovascular and cerebrovascular diseases. For instance, flavonoids can exert vasodilatory effects *in vitro* by regulating eNOS or Ca^{2+} channels (Tang et al., 2021). Phenolic acids protect the blood brain barrier through MMP-9 inhibition and anti-inflammation (Zhang & Song et al., 2018). Saponins have the pharmacological effects of anti-atherosclerosis, myocardial protection, and antithrombosis (Li et al., 2015). For example, HSYA, as the marker compound of safflower, has been widely used for the treatment of cerebrovascular and cardiovascular diseases due to its property of promoting blood circulation and removing blood stasis (Yang et al., 2020). Formononetin could alleviate the development of atherosclerosis by regulating the interaction between KLF4 and SRA (Ma et al., 2020). Amygdalin was reported to have the effect of reducing the development of atherosclerosis by inhibiting inflammatory reaction and promoting the immune regulation function of T cells (Deng et al., 2011). Naringin, a major compound of flavanone, which can be extracted from many CMM herbs, has the effects of anti-atherosclerosis, anti-hypertension, and myocardial protection (Hsueh et al., 2016; Sun et al., 2019). Isoliquiritigenin is a flavonoid compound from *Glycyrrhiza glabra* that has been proven to attenuate atherosclerosis lesion and decrease blood lipid level by inhibiting TRPC5 channel (Qi et al., 2020). Also, it has been reported that hesperidin prevents the redox imbalance induced by hyperlipidemia (Kumar, Akhtar, & Rizvi, 2020). *In vitro* and *in vivo* experiments showed that ferulic acid has antithrombotic, hypolipidemic activities, and so on (Choi et al., 2018; Kamal-Eldin et al., 2000; Zhu & Zhang, 2014).

3.3. Identification of metabolites from XFZYD in serum

Enzymes play an important role in the metabolism of CMM compounds. It can metabolize prototype compounds derived from the studied formula into active metabolites, contributing to the treatment of diseases. β-Glucosidase is abundant enzyme in intestinal, which can easily transform glycoside into aglycone by deglycosylation reaction (Yan et al., 2018). In liver, liver microsomal enzymes can metabolize prodrug into metabolites through Ⅰ and Ⅱ phase metabolism (Zeng et al., 2018). By analyzing the chromatograms of the blank serum and dosed serum (Fig. 3), a total of 151 metabolites were tentatively identified by the Metabolyxn (Masslynx V4.1 software) and detailed MS data (Table 2 and Supplementary Table S2). There were 71, 53, 14, and 13 metabolites transformed from flavanones, saponins, phenolic acids and other compounds, respectively. The network was adopted to display the relationship between prototype compounds and metabolites,

Table 1
MS data of prototype compounds from XFZYD in serum by UPLC-Q-TOF/MS.

No.	Compounds	t_R (min)	Formula	Negative ion mode (−)	Positive ion mode (+)
				$[M-H]^-$, (m/z)	$[M+H]^+$, (m/z)
P1	PHBA	4.080	$C_7H_6O_3$	137.0239	–
P2	HSYA	5.512	$C_{27}H_{32}O_{16}$	611.1612	613.1769
P3	Amygdalin	6.200	$C_{20}H_{27}NO_{11}$	456.1506	458.1662
P4	PHCA	7.532	$C_9H_8O_3$	163.0395	–
P5	Albiflorin	7.922	$C_{23}H_{28}O_{11}$	525.1608 *	481.1710
P6	Paeoniflorin	8.739	$C_{23}H_{28}O_{11}$	525.1608 *	498.1985 #
P7	Ferulic acid	9.182	$C_{10}H_{10}O_4$	193.0501	–
P8	Liquiritin	10.355	$C_{21}H_{22}O_9$	417.1186	419.1342
P9	Isoquercitrin	10.698	$C_{21}H_{20}O_{12}$	463.0877	465.1033
P10	Narirutin	12.73	$C_{27}H_{32}O_{14}$	579.1714	581.1870
P11	β-Ecdysterone	12.814	$C_{27}H_{44}O_7$	479.3009	481.3165
P12	Naringin	13.474	$C_{27}H_{32}O_{14}$	579.1714	581.1870
P13	Rhoifolin	13.711	$C_{27}H_{30}O_{14}$	577.1557	579.1714
P14	Hesperidin	14.372	$C_{28}H_{34}O_{15}$	609.1819	611.1976
P15	Neohesperidin	15.112	$C_{28}H_{34}O_{15}$	609.1819	611.1976
P16	Liquiritigenin	15.521	$C_{15}H_{12}O_4$	255.0657	257.0814
P17	Naringenin	18.424	$C_{15}H_{12}O_5$	271.0606	273.0763
P18	Platycodin D	19.254	$C_{57}H_{92}O_{28}$	1223.5697	1225.5853
P19	Isoliquiritigenin	20.214	$C_{15}H_{12}O_4$	255.0657	257.0814
P20	Formononetin	20.776	$C_{16}H_{12}O_4$	267.0657	269.0814
P21	Ginsenoside-Ro	21.398	$C_{48}H_{76}O_{19}$	955.4903	957.5059
P22	18β-Glycyrrhizic acid	22.356	$C_{42}H_{62}O_{16}$	821.3960	823.4116
P23	Nobiletin	23.130	$C_{21}H_{22}O_8$	–	403.1393
P24	Saikosaponin A	24.174	$C_{42}H_{68}O_{13}$	779.4582	781.4738

P = prototype compound, "–" undetected, "*" $[M-H+HCOOH]^-$, "#" $[M+NH_4]^+$.

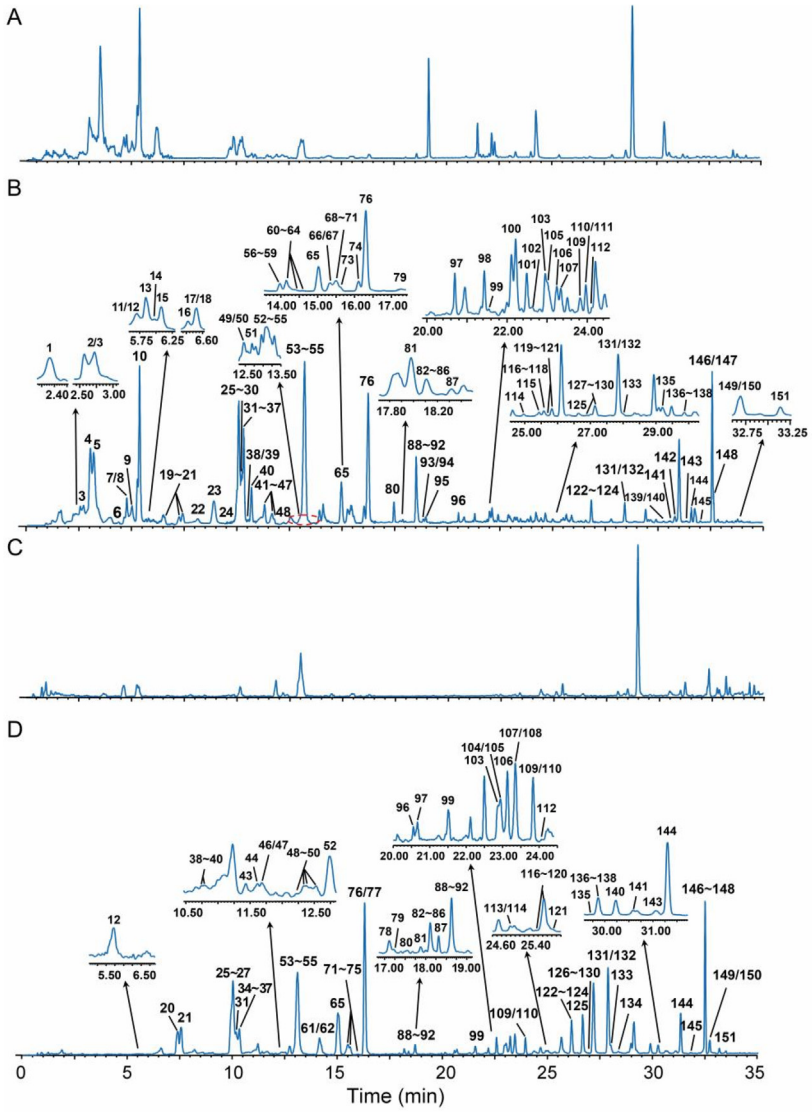

Fig. 3. Extracted ion chromatograms of metabolites of serum samples. Blank serum sample (A) and dosed serum sample (B) in negative mode; Blank serum sample (C) and dosed serum sample (D) in positive mode.

and 24 prototype compounds (P1–P24) identified from XFZYD have been modified into 151 metabolites, which was shown in Fig. 4. Interestingly, it can be drawn that one prototype compound can be metabolized into the different metabolites, the different prototype compounds can be metabolized into the same metabolite. $M_{10\text{-}8}$ taken as a typical example was simultaneously produced by narirutin, naringin, and neohesperidin *in vivo*. Meanwhile, narirutin, naringin, and neohesperidin can be metabolized into the different metabolites besides $M_{10\text{-}8}$, respectively.

As follows, we introduced the identified metabolites and summarized metabolic pathways of prototype compounds derived from the different characteristics of structures.

3.3.1. Identification of metabolites from flavanones

In this study, 13 prototype flavonoids were identified in rat' serum after oral administration of XFZYD, which were mainly originated from Honghua, Gancao, Zhiqiao, and Danggui. With the aid of Metabolyxn (Masslynx V4.1 software), 71 metabolites from flavonoids were identified (Table 2 and Supplementary Table S2), which were derived from P2 (one metabolite), P8 (10 metabolites), P9 (six metabolites), P10 (11 metabolites), P12 (six metabolites), P13 (18 metabolites), P14 (five metabolites), P15 (11 metabolites), P16 (eight metabolites), P17 (four metabolites), P19 (nine metabolites), P20 (five metabolites) and P23 (two metabolites), respectively. By studying the metabolic pathways in detail, we found that flavonoids mainly undergo glucuronidation, sulfation deglycosylation, demethylation, and deoxidation reactions. For example, neohesperidin (P15) was modified into eleven metabolites ($M_{15\text{-}1}$–$M_{15\text{-}11}$) through above-mentioned metabolic pathways (Fig. 5).

Glucuronidation: $M_{15\text{-}4}$ showed a quasi-molecular ion at *m*/*z* 785.2145 in the negative ion mode, 176 Da heavier than neohesperidin at *m*/*z* 609.1842, suggesting that glucuronidation reaction has happened to neohesperidin. Fragment ions of $M_{15\text{-}4}$ at *m*/*z* 301.0714, 151.0059, 149.0621, and 175.0255 were detected, whose fragmentation characteristics were similar to neohesperidin. The characteristic fragment ion of glucuronic acid was monitored at *m*/*z* 175.0255. This result indicated that the occurrence of glucuronidation conjugation to neohesperidin.

Deglycosylation + Glucuronidation: In the negative ion mode, $M_{15\text{-}7}$, $M_{15\text{-}8}$, and $M_{15\text{-}9}$ showed quasi-molecular ion at *m*/*z* 301.0722 and were identified as aglycone of neohesperidin, suggesting that deglycosylation reaction has occurred to neohes-

Table 2
MS data and metabolic pathways of metabolites after oral administration of XFZYD by UPLC-Q-TOF/MS.

Prototypes	Metabolic pathways	No.	t_R (min)	Peak No.	Negative ion mode (−)	Positive ion mode (+)	Formula
					$[M-H]^-$, (m/z)	$[M+H]^+$, (m/z)	
PHBA	Parent	P_1	3.99	–	137.0242	–	$C_7H_6O_3$
	Hydroxylation + Methylation	M_{1-1}	5.74	11	167.0350	–	$C_8H_8O_4$
	Hydroxylation	M_{1-2}	6.04	14	153.0195	–	$C_7H_6O_4$
HSYA	Parent	P_2	5.51	–	611.1616	–	$C_{27}H_{32}O_{16}$
	Deoxidation	M_{2-1}	11.43	42	595.1682	–	$C_{27}H_{32}O_{15}$
Amygdalin	Parent	P_3	6.13	–	456.1506	480.1478 #	$C_{20}H_{27}NO_{11}$
	Deglycosylation (glucose)	M_{3-1}	7.42	20	294.0985	318.0961 #	$C_{14}H_{17}NO_6$
		M_{3-2}	7.58	21	294.0984	318.0962 #	$C_{14}H_{17}NO_6$
	Deglycosylation (2 × glucose) + Sulfate conjugation	M_{3-3}	8.90	23	212.0025	–	$C_8H_7NO_4S$
PHCA	Parent	P_4	7.51	–	163.0402	–	$C_9H_8O_3$
	Hydroxylation + Sulfation conjugation	M_{4-1}	4.90	9	258.9922	–	$C_9H_8O_7S$
	Sulfate conjugation	M_{4-2}	2.65	2	242.9968	–	$C_9H_8O_6S$
		M_{4-3}	4.77	8	242.9970	–	$C_9H_8O_6S$
		M_{4-4}	5.84	13	242.9969	–	$C_9H_8O_6S$
		M_{4-5}	6.07	15	242.9969	–	$C_9H_8O_6S$
Albiflorin	Parent	P_5	7.91	–	525.1614 *	503.1537 #	$C_{23}H_{28}O_{11}$
	De-benzoic acid	M_{5-1}	5.74	12	359.1338	383.1314 #	$C_{16}H_{24}O_9$
	De-benzoic acid + Dehydration	M_{5-2}	10.65	38	341.1243	365.1212 #	$C_{16}H_{22}O_8$
	De-benzoic acid + Acetylation	M_{5-3}	10.80	40	401.1451	425.1432 #	$C_{18}H_{26}O_{10}$
Paeoniflorin	Parent	P_6	8.72	–	525.1609 *	503.1525 #	$C_{23}H_{28}O_{11}$
	De-debenzoylpaeoniflorin + Glucuronide conjugation	M_{6-1}	2.38	1	343.0662 *	–	$C_{13}H_{14}O_8$
	De-debenzoylpaeoniflorin + Hydroxylation + sulfate conjugation	M_{6-2}	2.73	3	262.9869 *	–	$C_7H_6O_6S$
	De-debenzoylpaeoniflorin + Sulfate conjugation	M_{6-3}	3.06	4	246.9924 *	–	$C_7H_6O_5S$
Ferulic acid	Parent	P_7	9.18	–	193.0507	–	$C_{10}H_{10}O_4$
	Glucuronide conjugation	M_{7-1}	4.34	6	369.0823	–	$C_{16}H_{18}O_{10}$
		M_{7-2}	6.57	18	369.0834	–	$C_{16}H_{18}O_{10}$
	Sulfate conjugation	M_{7-3}	3.13	5	273.0078	–	$C_{10}H_{10}O_7S$
		M_{7-4}	5.38	10	273.0081	–	$C_{10}H_{10}O_7S$
		M_{7-5}	6.41	16	273.0080	–	$C_{10}H_{10}O_7S$
		M_{7-6}	6.56	17	273.0080	–	$C_{10}H_{10}O_7S$
	Demethylation + Sulfate conjugation	M_{7-7}	4.90	9	258.9918	–	$C_9H_8O_7S$
	Demethylation + Deoxidation + Sulfate conjugation	M_{7-8}	2.65	2	242.9968	–	$C_9H_8O_6S$
		M_{7-9}	4.66	7	242.9973	–	$C_9H_8O_6S$
		M_{7-10}	4.77	8	242.9970	–	$C_9H_8O_6S$
		M_{7-11}	6.07	15	242.9968	–	$C_9H_8O_6S$
Liquiritin	Parent	P_8	10.32	–	417.1195	419.1353	$C_{21}H_{22}O_9$
	Glucuronide conjugation	M_{8-1}	6.61	19	593.1511	–	$C_{27}H_{30}O_{15}$
		M_{8-2}	10.19	31	593.1508	595.1645	$C_{27}H_{30}O_{15}$
	Hydroxylation + Dehydrogenation	M_{8-3}	10.04	25	431.0979	433.1131	$C_{21}H_{20}O_{10}$
		M_{8-4}	10.36	35	431.0979	433.1134	$C_{21}H_{20}O_{10}$
	Deglycosylation (glucose) + Hydroxylation + Glucuronide conjugation	M_{8-5}	13.11	54	447.0931	449.1082	$C_{21}H_{20}O_{11}$
	Hydroxylation + Methylation	M_{8-6}	17.54	80	447.1289	449.1444	$C_{22}H_{24}O_{10}$
	Hydroxylation + Sulfation conjugation	M_{8-7}	14.31	63	513.0705	–	$C_{21}H_{22}O_{13}S$
	Deglycosylation (glucose) + Methylation	M_{8-8}	18.62	88	269.0817	271.0978	$C_{16}H_{14}O_4$
	Deglycosylation (glucose) + Sulfate conjugation	M_{8-9}	12.41	49	335.0229	337.0376	$C_{15}H_{12}O_7S$
		M_{8-10}	18.14	85	335.0230	337.0384	$C_{15}H_{12}O_7S$
Isoquercitrin	Parent	P_9	10.69	–	463.0880	465.102	$C_{21}H_{20}O_{12}$
	Methylation + Deoxidation	M_{9-1}	13.98	56	461.1090	–	$C_{22}H_{22}O_{11}$
		M_{9-2}	14.15	60	461.1086	–	$C_{22}H_{22}O_{11}$
		M_{9-3}	18.98	93	461.1088	–	$C_{22}H_{22}O_{11}$
	Deoxidation	M_{9-4}	15.33	66	447.0936	–	$C_{21}H_{20}O_{11}$
	Deoxidation + Sulfate conjugation	M_{9-5}	10.11	30	527.0497	–	$C_{21}H_{20}O_{14}S$
		M_{9-6}	10.26	33	527.0498	–	$C_{21}H_{20}O_{14}S$
Narirutin	Parent	P_{10}	12.72	–	579.1718	581.1868	$C_{27}H_{32}O_{14}$
	Deglycosylation (rhamnose) + Dehydrogenation	M_{10-1}	10.04	26	431.0979	433.1131	$C_{21}H_{20}O_{10}$
		M_{10-2}	10.36	36	431.0979	433.1134	$C_{21}H_{20}O_{10}$
	Deglycosylation (rutinose) + Glucuronide conjugation	M_{10-3}	13.11	54	447.0931	449.1082	$C_{21}H_{20}O_{11}$
	Hydroxylation	M_{10-4}	10.72	39	595.1658	597.181	$C_{27}H_{32}O_{15}$
		M_{10-5}	11.43	43	595.1677	–	$C_{27}H_{32}O_{15}$
	Hydroxylation + Dehydrogenation	M_{10-6}	18.11	82	593.1506	595.1644	$C_{27}H_{30}O_{15}$
	Hydroxylation + Methylation	M_{10-7}	17.23	79	609.1833	611.1979	$C_{28}H_{34}O_{15}$
	Deglycosylation (rutinose) + Hydroxylation + Methylation	M_{10-8}	13.04	52	301.0722	303.0875	$C_{16}H_{14}O_6$
		M_{10-9}	13.23	55	301.0717	303.0872	$C_{16}H_{14}O_6$
		M_{10-10}	14.23	62	301.0722	303.0883	$C_{16}H_{14}O_6$
	Methylation	M_{10-11}	14.01	58	593.1874	–	$C_{28}H_{34}O_{14}$

(*continued on next page*)

Table 2 (*continued*)

Prototypes	Metabolic pathways	No.	t_R (min)	Peak No.	Negative ion mode (−)	Positive ion mode (+)	Formula
					$[M-H]^-$, (m/z)	$[M+H]^+$, (m/z)	
β-Ecdysterone	Parent	P_{11}	12.82	–	525.3080 *	–	$C_{27}H_{44}O_7$
	Methylation	M_{11-1}	22.44	100	539.3206 *	–	$C_{28}H_{46}O_7$
	Reduction + Deoxidation	M_{11-2}	22.48	101	511.3267 *	–	$C_{27}H_{46}O_6$
	Demethylation + Deoxidation	M_{11-3}	22.63	102	495.2962 *	–	$C_{26}H_{42}O_6$
	Acetylation	M_{11-4}	23.97	111	567.3167 *	–	$C_{29}H_{46}O_8$
Naringin	Parent	P_{12}	13.47	–	579.1719	581.1863	$C_{27}H_{32}O_{14}$
	Deglycosylation (rhamnose) + Dehydrogenation	M_{12-1}	10.04	26	431.0979	433.1131	$C_{21}H_{20}O_{10}$
		M_{12-2}	10.36	36	431.0979	433.1134	$C_{21}H_{20}O_{10}$
	Deglycosylation (neohesperidose) + Glucuronide conjugation	M_{12-3}	13.11	54	447.0931	449.1082	$C_{21}H_{20}O_{11}$
	Hydroxylation + Dehydrogenation	M_{12-4}	18.11	83	593.1506	595.1644	$C_{27}H_{30}O_{15}$
	Deglycosylation (neohesperidose) + Hydroxylation + Methylation	M_{12-5}	13.04	52	301.0722	303.0875	$C_{16}H_{14}O_6$
	Methylation	M_{12-6}	14.01	59	593.1874	–	$C_{28}H_{34}O_{14}$
Rhoifolin	Parent	P_{13}	13.71	–	577.1590	579.1697	$C_{27}H_{30}O_{14}$
	Deglycosylation (neohesperidose) + Hydroxylation + Glucuronide conjugation	M_{13-1}	12.33	48	461.0726	463.0879	$C_{21}H_{18}O_{12}$
	Deglycosylation (rhamnose) + Hydroxylation + Methylation	M_{13-2}	14.15	61	461.1086	–	$C_{22}H_{22}O_{11}$
		M_{13-3}	13.98	57	461.1090	–	$C_{22}H_{22}O_{11}$
		M_{13-4}	18.98	94	461.1088	–	$C_{22}H_{22}O_{11}$
		M_{13-5}	19.10	95	461.1084	–	$C_{22}H_{22}O_{11}$
	Deglycosylation (neohesperidose) + Hydroxylation + Sulfation conjugation	M_{13-6}	9.86	24	364.9967	–	$C_{15}H_{10}O_9S$
	Deglycosylation (rhamnose) + Hydroxylation + Sulfation conjugation	M_{13-7}	10.09	28	527.0500	–	$C_{21}H_{20}O_{14}S$
		M_{13-8}	10.25	32	527.0500	–	$C_{21}H_{20}O_{14}S$
	Deglycosylation (rhamnose) + Hydroxylation	M_{13-9}	15.33	67	447.0936	–	$C_{21}H_{20}O_{11}$
	Deglycosylation (rhamnose) + Methylation	M_{13-10}	18.64	91	445.1133	447.1294	$C_{22}H_{22}O_{10}$
	Deglycosylation (rhamnose)	M_{13-11}	10.04	26	431.0979	433.113	$C_{21}H_{20}O_{10}$
		M_{13-12}	10.36	36	431.0979	–	$C_{21}H_{20}O_{10}$
		M_{13-13}	15.62	72	–	433.1136	$C_{21}H_{20}O_{10}$
		M_{13-14}	16.30	77	–	433.113	$C_{21}H_{20}O_{10}$
	Deglycosylation (rhamnose) + Reduction	M_{13-15}	11.57	45	433.1135	–	$C_{21}H_{22}O_{10}$
		M_{13-16}	17.09	78	–	435.129	$C_{21}H_{22}O_{10}$
	Deglycosylation (rhamnose) + Sulfate conjugation	M_{13-17}	12.54	51	511.0547	–	$C_{21}H_{20}O_{13}S$
		M_{13-18}	8.22	22	511.0553	–	$C_{21}H_{20}O_{13}S$
Hesperidin	Parent	P_{14}	14.37	–	609.1814	611.1979	$C_{28}H_{34}O_{15}$
	Deglycosylation (rutinose) + 2 × Glucuronide conjugation	M_{14-1}	11.23	41	653.1345	–	$C_{28}H_{30}O_{18}$
	Glucuronide conjugation	M_{14-2}	11.60	46	785.2145	787.2285	$C_{34}H_{42}O_{21}$
	Deglycosylation (rhamnose) + Dehydrogenation	M_{14-3}	14.15	61	461.1087	463.1242	$C_{22}H_{22}O_{11}$
	Deglycosylation (rutinose) + Glucuronide conjugation	M_{14-4}	15.03	65	477.1036	479.1185	$C_{22}H_{22}O_{12}$
	Dehydrogenation + Demethylation	M_{14-5}	18.11	82	593.1506	595.1644	$C_{27}H_{30}O_{15}$
Neohesperidin	Parent	P_{15}	15.09	–	609.1842	611.1967	$C_{28}H_{34}O_{15}$
	Deglycosylation (neohesperidose) + 2 × Glucuronide conjugation	M_{15-1}	11.23	41	653.1345	–	$C_{28}H_{30}O_{18}$
	Demethylation	M_{15-2}	11.43	43	595.1677	597.1825	$C_{27}H_{32}O_{15}$
	Deglycosylation (rhamnose) + Dehydrogenation	M_{15-3}	14.15	61	461.1087	463.1241	$C_{22}H_{22}O_{11}$
	Glucuronide conjugation	M_{15-4}	11.60	47	785.2145	787.2269	$C_{34}H_{42}O_{21}$
	Deglycosylation (neohesperidose) + Glucuronide conjugation	M_{15-5}	15.03	65	477.1036	479.1185	$C_{22}H_{22}O_{12}$
		M_{15-6}	15.47	70	477.1034	–	$C_{22}H_{22}O_{12}$
	Deglycosylation (neohesperidose)	M_{15-7}	13.04	52	301.0722	303.0876	$C_{16}H_{14}O_6$
		M_{15-8}	13.23	55	301.0717	303.087	$C_{16}H_{14}O_6$
		M_{15-9}	14.23	62	301.0722	303.0882	$C_{16}H_{14}O_6$
	Deoxidation	M_{15-10}	14.01	59	593.1874	–	$C_{28}H_{34}O_{14}$
	Deglycosylation (rhamnose) + Sulfate conjugation	M_{15-11}	14.58	64	543.0828	–	$C_{22}H_{24}O_{14}S$
Liquiritigenin	Parent	P_{16}	15.51	–	255.0659	257.0822	$C_{15}H_{12}O_4$
	Glucuronide conjugation	M_{16-1}	10.04	27	431.0979	433.1131	$C_{21}H_{20}O_{10}$
		M_{16-2}	10.36	37	431.0979	433.1134	$C_{21}H_{20}O_{10}$
	Hydroxylation	M_{16-3}	15.38	68	271.0621	–	$C_{15}H_{12}O_5$
	Hydroxylation + Glucuronide conjugation	M_{16-4}	10.09	29	447.0932	–	$C_{21}H_{20}O_{11}$
		M_{16-5}	13.11	54	447.0931	449.1082	$C_{21}H_{20}O_{11}$
	Methylation	M_{16-6}	18.62	88	269.0817	271.0978	$C_{16}H_{14}O_4$
	Sulfate conjugation	M_{16-7}	11.55	44	335.0225	337.0385	$C_{15}H_{12}O_7S$
		M_{16-8}	12.47	50	335.0229	337.0376	$C_{15}H_{12}O_7S$
Naringenin	Parent	P_{17}	18.42	–	271.0602	273.0771	$C_{15}H_{12}O_5$
	Glucuronide conjugation	M_{17-1}	13.13	54	447.0930	449.1082	$C_{21}H_{20}O_{11}$
	Sulfate conjugation	M_{17-2}	15.40	69	351.0183	353.0337	$C_{15}H_{12}O_8S$
	Deoxidation + Sulfate conjugation	M_{17-3}	18.15	85	335.0230	337.0384	$C_{15}H_{12}O_7S$
	Methylation + Deoxidation	M_{17-4}	18.62	88	269.0817	271.0978	$C_{16}H_{14}O_4$
Platycodin D	Parent	P_{18}	19.25	–	1223.5681	1225.5792	$C_{57}H_{92}O_{28}$
	Deglycosylation (apiose + xylose + rhamnose + arabinose)	M_{18-1}	21.40	98	681.3850	–	$C_{36}H_{58}O_{12}$
	Deglycosylation (apiose) + Methylation + Deoxidation	M_{18-2}	30.90	142	1089.5479	–	$C_{53}H_{86}O_{23}$

Table 2 (*continued*)

Prototypes	Metabolic pathways	No.	t_R (min)	Peak No.	Negative ion mode (−)	Positive ion mode (+)	Formula
					$[M-H]^-$, (*m*/*z*)	$[M+H]^+$, (*m*/*z*)	
Isoliquiritigenin	Parent	P_{19}	20.21	–	255.0669	257.0823	$C_{15}H_{12}O_4$
	Hydroxylation + Sulfation conjugation	M_{19-1}	10.27	34	351.0177	353.0334	$C_{15}H_{12}O_8S$
	Glucuronide conjugation	M_{19-2}	10.36	37	431.0979	433.1134	$C_{21}H_{20}O_{10}$
	Sulfate conjugation	M_{19-3}	12.47	50	335.0229	337.0376	$C_{15}H_{12}O_7S$
	Hydroxylation + Glucuronide conjugation	M_{19-4}	13.11	54	447.0931	449.1082	$C_{21}H_{20}O_{11}$
		M_{19-5}	15.51	71	447.0931	449.1086	$C_{21}H_{20}O_{11}$
	Glucuronide conjugation	M_{19-6}	15.62	73	431.0982	433.1137	$C_{21}H_{20}O_{10}$
		M_{19-7}	16.23	76	431.0978	433.113	$C_{21}H_{20}O_{10}$
	Sulfate conjugation	M_{19-8}	18.16	86	335.0230	337.0384	$C_{15}H_{12}O_7S$
	Methylation	M_{19-9}	18.62	89	269.0817	271.0978	$C_{16}H_{14}O_4$
Formononetin	Parent	P_{20}	20.77	–	267.0666	269.0825	$C_{16}H_{12}O_4$
	Glucuronide conjugation	M_{20-1}	16.11	74	443.0978	445.1135	$C_{22}H_{20}O_{10}$
	Hydroxylation + Glucuronide conjugation	M_{20-2}	13.10	53	459.0933	461.108	$C_{22}H_{20}O_{11}$
		M_{20-3}	17.88	81	459.0924	461.108	$C_{22}H_{20}O_{11}$
	Reduction	M_{20-4}	18.62	90	269.0817	271.0978	$C_{16}H_{14}O_4$
	Sulfate conjugation	M_{20-5}	18.68	92	347.0228	349.0386	$C_{16}H_{12}O_7S$
Ginsenoside-Ro	Parent	P_{21}	21.39	–	955.4894	–	$C_{48}H_{76}O_{19}$
	Deglycosylation (glucose) + Deglucuronidation + 2 × Dehydrogenation	M_{21-1}	20.69	97	613.3737	615.3871	$C_{36}H_{54}O_8$
	Deglycosylation (glucose) + Hydroxylation + Dehydrogenation	M_{21-2}	25.43	115	807.4169	–	$C_{42}H_{64}O_{15}$
	Deglycosylation (glucose) + Deglucuronidation + Hydroxylation + Dehydrogenation	M_{21-3}	30.22	139	631.3857	–	$C_{36}H_{56}O_9$
18β-Glycyrrhizic acid	Parent	P_{22}	22.37	–	821.3950	823.4107	$C_{42}H_{62}O_{16}$
	2 × Deglucuronidation + 3 × Hydroxylation	M_{22-1}	23.34	107	517.3167	519.3307	$C_{30}H_{46}O_7$
	2 × Deglucuronidation + Demethylation + Hydroxylation	M_{22-2}	24.13	112	471.3106	473.3261	$C_{29}H_{44}O_5$
		M_{22-3}	25.58	116	471.3114	473.3272	$C_{29}H_{44}O_5$
		M_{22-4}	25.73	119	471.3110	473.3272	$C_{29}H_{44}O_5$
		M_{22-5}	26.10	122	471.3113	473.327	$C_{30}H_{44}O_5$
		M_{22-6}	26.65	125	471.3113	473.3267	$C_{29}H_{44}O_5$
		M_{22-7}	30.59	141	471.3115	473.3269	$C_{29}H_{44}O_5$
	Deglucuronidation + Demethylation + Hydroxylation	M_{22-8}	20.62	96	647.3424	649.3581	$C_{35}H_{52}O_{11}$
	2 × Deglucuronidation + Demethylation	M_{22-9}	23.38	108	–	457.332	$C_{29}H_{44}O_4$
		M_{22-10}	30.23	140	455.3157	457.3316	$C_{29}H_{44}O_4$
		M_{22-11}	31.01	143	455.3166	457.3317	$C_{29}H_{44}O_4$
		M_{22-12}	31.31	144	455.3159	457.332	$C_{29}H_{44}O_4$
	2 × Deglucuronidation + Dehydrogenation	M_{22-13}	28.34	134	–	469.3318	$C_{30}H_{44}O_4$
	Deglucuronidation + Deoxidation + Dehydrogenation	M_{22-14}	23.88	110	659.3431	661.3585	$C_{36}H_{52}O_{11}$
	Hydroxylation	M_{22-15}	18.31	87	837.3928	839.4043	$C_{42}H_{62}O_{17}$
	2 × Deglucuronidation + Hydroxylation + Dehydrogenation	M_{22-16}	25.83	121	483.3111	485.3264	$C_{30}H_{44}O_5$
		M_{22-17}	27.13	128	483.3103	485.3266	$C_{30}H_{44}O_5$
		M_{22-18}	27.99	133	483.3132	485.3272	$C_{30}H_{44}O_5$
		M_{22-19}	29.86	136	483.3112	485.3268	$C_{30}H_{44}O_5$
	Deglucuronidation + Hydroxylation + Dehydrogenation	M_{22-20}	22.96	104	–	661.3583	$C_{36}H_{52}O_{11}$
	2 × Deglucuronidation + Hydroxylation + Sulfation conjugation	M_{22-21}	22.93	103	565.2838	567.2986	$C_{30}H_{46}O_8S$
		M_{22-22}	23.16	106	565.2840	567.2985	$C_{30}H_{46}O_8S$
	2 × Deglucuronidation + Hydroxylation	M_{22-23}	23.85	109	485.3260	487.3422	$C_{30}H_{46}O_5$
		M_{22-24}	24.98	114	485.3271	487.3424	$C_{30}H_{46}O_5$
		M_{22-25}	25.64	117	485.3273	487.3425	$C_{30}H_{46}O_5$
		M_{22-26}	26.12	123	485.3271	487.3426	$C_{30}H_{46}O_5$
		M_{22-27}	27.17	129	485.3259	487.3423	$C_{30}H_{46}O_5$
		M_{22-28}	27.85	131	485.3275	487.3426	$C_{30}H_{46}O_5$
		M_{22-29}	29.87	138	485.3259	487.3424	$C_{30}H_{46}O_5$
	Deglucuronidation + Hydroxylation	M_{22-30}	21.51	99	661.3586	663.3733	$C_{36}H_{54}O_{11}$
	2 × Deglucuronidation	M_{22-31}	32.40	146	469.3322	471.3491	$C_{30}H_{46}O_4$
		M_{22-32}	32.69	149	469.3313	471.3472	$C_{30}H_{46}O_4$
	Deglucuronidation	M_{22-33}	26.81	127	645.3626	647.3785	$C_{36}H_{54}O_{10}$
	Deglucuronidation + Sulfate conjugation	M_{22-34}	22.99	105	725.3210	727.3356	$C_{36}H_{54}O_{13}S$
Nobiletin	Parent	P_{23}	23.12	–	–	403.1392	$C_{21}H_{22}O_8$
	Hydroxylation	M_{23-1}	16.22	75	–	419.1338	$C_{21}H_{22}O_9$
	Hydroxylation + Glucuronide conjugation	M_{23-2}	18.11	84	–	595.1641	$C_{27}H_{30}O_{15}$
Saikosaponin A	Parent	P_{24}	24.17	–	779.4595	–	$C_{42}H_{68}O_{13}$
	Deglycosylation (glucose + rhamnose) + Dehydrogenation	M_{24-1}	32.40	147	469.3332	471.3491	$C_{30}H_{46}O_4$
		M_{24-2}	32.47	148	469.3318	471.3492	$C_{30}H_{46}O_4$
		M_{24-3}	32.69	150	469.3313	471.3472	$C_{30}H_{46}O_4$
		M_{24-4}	33.15	151	469.3311	471.3474	$C_{30}H_{46}O_4$
	Deglycosylation	M_{24-5}	24.89	113	–	487.3425	$C_{30}H_{46}O_5$
	(glucose + rhamnose) + Hydroxylation + Dehydrogenation	M_{24-6}	25.64	118	485.3273	487.3425	$C_{30}H_{46}O_5$
		M_{24-7}	26.12	124	485.3271	487.3426	$C_{30}H_{46}O_5$
		M_{24-8}	26.70	126	–	487.3424	$C_{30}H_{46}O_5$

(*continued on next page*)

Table 2 (*continued*)

Prototypes	Metabolic pathways	No.	t_R (min)	Peak No.	Negative ion mode (−)	Positive ion mode (+)	Formula
					$[M-H]^-$, (*m*/*z*)	$[M+H]^+$, (*m*/*z*)	
		M_{24-9}	27.17	130	485.3262	487.3423	$C_{30}H_{46}O_5$
		M_{24-10}	27.85	132	485.3257	487.3426	$C_{30}H_{46}O_5$
		M_{24-11}	29.18	135	485.3266	487.341	$C_{30}H_{46}O_5$
		M_{24-12}	29.86	137	485.3264	487.3424	$C_{30}H_{46}O_5$
	Deglycosylation (glucose + rhamnose)	M_{24-13}	25.75	120	471.3467	473.3642	$C_{30}H_{48}O_4$
	Deglycosylation (glucose + rhamnose) + 2 × Dehydrogenation	M_{24-14}	32.31	145	467.3164	469.3309	$C_{30}H_{44}O_4$

P = prototype compound, M = metabolite, "−" undetected, "*" $[M-H+HCOOH]^-$, "#" $[M+Na]^+$.

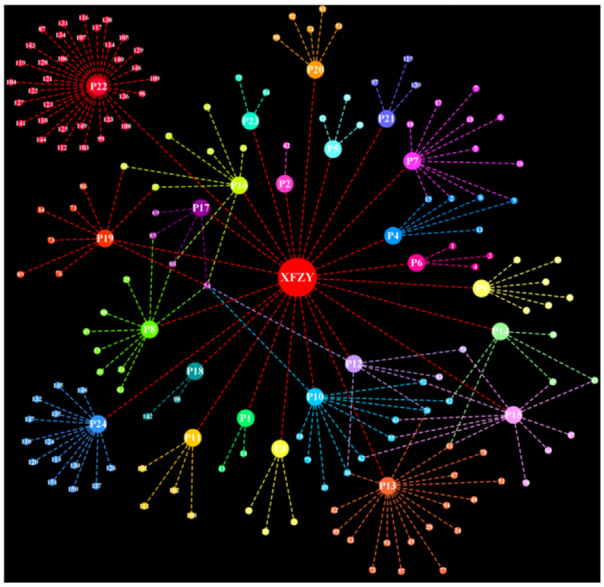

Fig. 4. Metabolic network of prototype compounds in XFZYD.

peridin by intestine microbiota (Lin et al., 2020). M_{15-5} and M_{15-6} showed quasi-molecular ion both at *m*/*z* 477.1034, indicating that glucuronidation has occurred at the different hydroxyl group of hesperetin. The fragment ions of M_{15-5} and M_{15-6} were detected at *m*/*z* 301.0721, 151.0040 and 149.0617, which were similar to that of neohesperidin. M_{15-1} was identified as a product derived from the successive glucuronidation reaction to hesperetin, whose quasi-molecular ion was found at *m*/*z* 653.1345.

Sulfation: As a sulfated product, M_{15-11} showed a quasi-molecular ion at *m*/*z* 543.0828 and fragment ions at *m*/*z* 463.1240, 301.0385, 151.0044, and 149.0606 in the negative ion mode, indicating that sulfation reaction has happened to the metabolite generated from neohesperidin by losing a rhamnose.

Demethylation: M_{15-2} was tentatively identified as a demethylated product by comparing the quasi-molecular ion between M_{15-2} and neohesperidin, whose gap was 14 Da in the negative ion mode.

In addition, M_{15-10} was metabolized by neohesperidin through deoxidation reaction by loss of oxygen (16 Da) and showed a quasi-molecular ion at *m*/*z* 593.1874 in the negative ion mode.

In general, illumination of the proposed metabolic pathway about neohesperidin paved the way for studying the metabolites of other flavonoids. The identified metabolites of flavonoids are displayed in Table 2 and Supplementary Table S2.

3.3.2. Identification of metabolites from saponins

Based on the information of chromatographic behavior and MS data, four prototype compounds from saponins primarily derived from Jiegeng, Chuanxiong, Gancao, and Chaihu, were identified by comparing with standards, which were transformed into 53 metabolites, including two metabolites from P18, three metabolites from P21, 34 metabolites from P22, and 14 metabolites from P24 (Table 2 and Supplementary Table S2). Hydrolyzation, dehydrogenation, and hydroxylation were found to happen in the process of saponins metabolism. Give an example about how to identify metabolites, saikosaponin A underwent the mentioned metabolic pathways to produce 14 metabolites (M_{24-1}–M_{24-14}) in negative ion mode.

Compared to the quasi-molecular ion of saikosaponin A at *m*/*z* 779.4595, that of M_{24-13} was found to lose 308 Da and detected at *m*/*z* 471.3467, indicating that glucose and rhamnose were sequentially hydrolyzed from saikosaponin A to produce aglycone. The fragment ion at *m*/*z* 453.3000 was generated from M_{24-13} by losing H_2O. The quasi-molecular ion of M_{24-1}–M_{24-4} at *m*/*z* 469.3318 and the fragment ion at *m*/*z* 451.3203 were observed, which was inferred that M_{24-1}–M_{24-4} were produced by dehydrogenation of M_{24-13}. The successive dehydrogenation to M_{24-13} produced M_{24-14}, whose quasi-molecular ion was monitored at *m*/*z* 467.3164 and a fragment ion at *m*/*z* 449.3234. The hydroxylation reaction occurred to M_{24-1}–M_{24-4}, which generated M_{24-5}-M_{24-12} with the quasi-molecular ion at *m*/*z* 485.3264.

3.3.3. Identification of metabolites from phenolic acids

As phenolic acids derived from Dihuang, Danggui, Chuanxiong, and Jiegeng, P1, P4, and P7 were metabolized into two, five, and 11 metabolites detected in the dosed serum, respectively (Table 2 and Supplementary Table S2). The prominent metabolic reactions were hydroxylation and methylation for the tested compounds. For example, M_{1-2} showed a quasi-molecular ion at *m*/*z* 153.0195, which was 16 Da more than that of PHBA at *m*/*z* 137.0242 and produced the main fragment ions at *m*/*z* 109.0293 in the MS spectra, indicating that hydroxylation reaction has happened to PHBA. M_{1-1} was metabolized from PHBA by the sequential reaction of hydroxylation (16 Da) and methylation (14 Da), whose quasi-molecular ion was detected at *m*/*z* 167.0350.

3.3.4. Identification of metabolites from other prototype compounds

Originated from Niuxi, Taoren, and Chishao, *β*-ecdysterone, amygdalin, albiflorin, and paeoniflorin were identified and modified into four, three, three, and three metabolites detected in the serum after oral administration of XFZYD (Table 2 and Supplementary Table S2). Methylation, demethylation, acetylation, reduction, glucuronide conjugation, and sulfate conjugation were summarized from the identified metabolites. Taking M_{11-1}–M_{11-4} metabolized from P11 as an example, M_{11-1} provided the quasi-molecular ion at *m*/*z* 539.3206, 14 Da more than that of *β*-ecdysterone at *m*/*z*

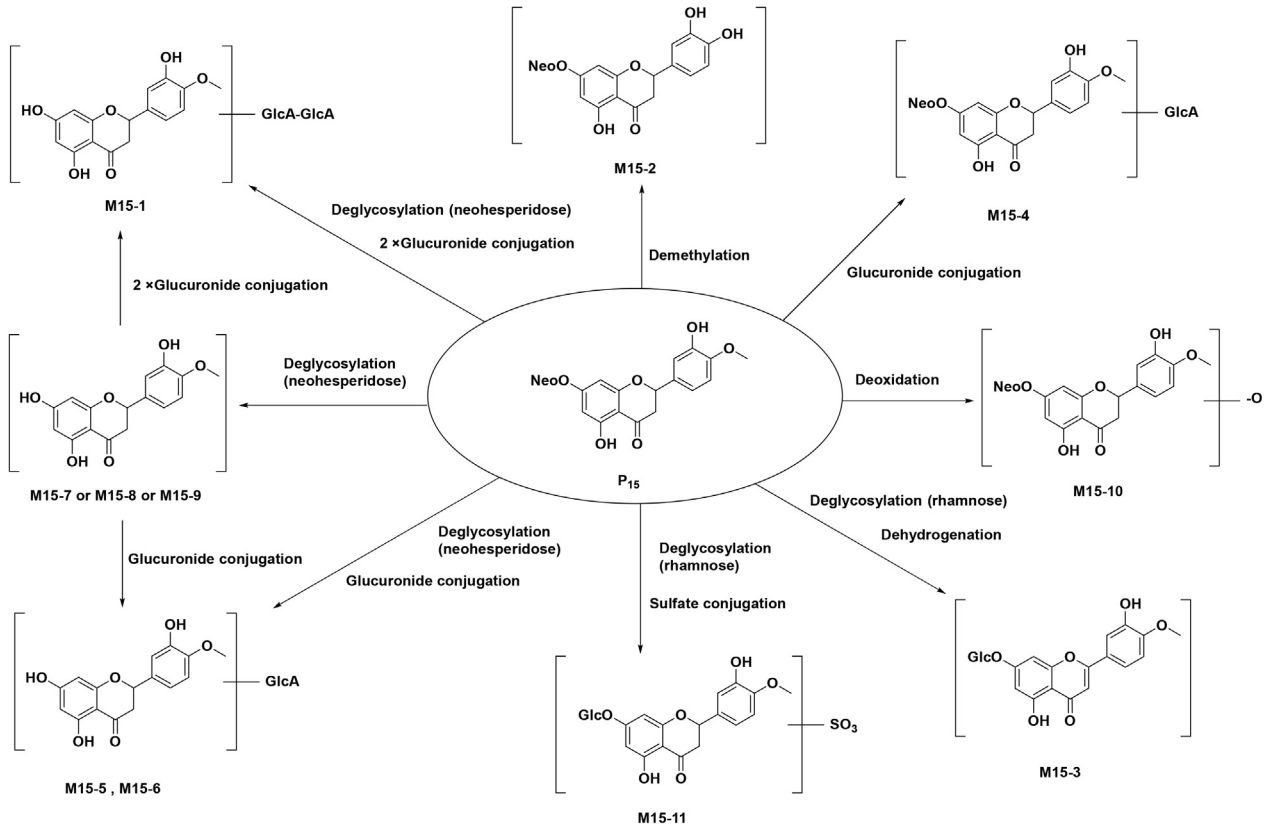

Fig. 5. Metabolic pathways of neohesperidin.

525.3080, suggesting that methylation reaction has occured. $M_{11\text{-}2}$ displayed a quasi-molecular ion at *m*/*z* 511.3267 and the fragment ions at *m*/*z* 351.2148, 333.2022, and 205.0889, showing that reduction and deoxidation reactions have happened to *β*-ecdysterone. $M_{11\text{-}3}$ was presumed to be the product of *β*-ecdysterone through demethylation and deoxidation reactions, whose quasi-molecular ion was monitored at *m*/*z* 495.2962. The quasi-molecular ion of $M_{11\text{-}4}$ was detected at *m*/*z* 567.3167, indicating that acetylation reaction has generated to *β*-ecdysterone.

4. Conclusion

In this study, we have established a rapid and effective UPLC-Q-TOF/MS method to identify the prototype compounds and their metabolites in rat' serum after intragastric administration of XFZYD, from which 175 compounds (24 prototype compounds and 151 metabolites) were identified and tentatively characterized. Metabolic rules of compounds with the different type of structures were summarized from the relationship between the prototype compounds and their metabolites. This study is meaningful for clarification of the absorbed compounds *in vivo*. Also, this study has demonstrated the feasibility of UPLC-Q-TOF/MS application in exploring the prototype compounds and metabolites originated from compound formula.

Declaration of Competing Interest

The authors declare that they have no known competing financial interests or personal relationships that could have appeared to influence the work reported in this paper.

Acknowledgments

This work was supported by National Natural Science Foundation of China (No. 81873192 and 81202877) and Postgraduate Research and Innovation Project of Tianjin (No. 2019YJSS197).

Appendix A. Supplementary data

Supplementary data to this article can be found online at https://doi.org/10.1016/j.chmed.2022.08.002.

References

Choi, J. H., Park, J. K., Kim, K. M., Lee, H. J., & Kim, S. (2018). *In vitro* and *in vivo* antithrombotic and cytotoxicity effects of ferulic acid. *Journal of Biochemical and Molecular Toxicology, 32*(1), e22004.

Deng, J. G., Li, C. Y., Wang, H. L., Hao, E. W., Du, Z. C., Bao, C. H., et al. (2011). Amygdalin mediates relieved atherosclerosis in apolipoprotein E deficient mice through the induction of regulatory T cells. *Biochemical and Biophysical Research Communications, 411*(3), 523–529.

Fan, H. S., Liu, S. J., Shen, W. X., Kang, A., Tan, J. N., Li, L., et al. (2020). Identification of the absorbed components and metabolites of Xiao-Ai-Jie-Du Decoction and their distribution in rats using ultra high-performance liquid chromatography/quadrupole time-of-flight mass spectrometry. *Journal of Pharmaceutical and Biomedical Analysis, 179*, 112984.

Feng, R., Zhao, Z. X., Ma, S. R., Guo, F., Wang, Y., & Jiang, J. D. (2018). Gut microbiota-regulated pharmacokinetics of berberine and active metabolites in beagle dogs after Oral administration. *Frontiers in Pharmacology, 9*, 214.

Feng, L. M., Chen, Y. Y., Xu, D. Q., Fu, R. J., Yue, S. J., Zhao, Q., et al. (2020). An integrated strategy for discovering effective components of Shaoyao Gancao Decoction for treating neuropathic pain by the combination of partial least-squares regression and multi-index comprehensive method. *Journal of Ethnopharmacology, 206*, 113050.

Fu, C. Y., Xia, Z., Liu, Y. H., Lu, H. M., Zhang, Z. M., Wang, Y., et al. (2016). Qualitative analysis of major constituents from XueFu ZhuYu Decoction using ultra high performance liquid chromatography with hybrid ion trap time-of-flight mass spectrometry. *Journal of Separation Science, 39*(17), 3457–3468.

Fu, C. Y., Wu, Q., Zhang, Z. M., Xia, Z., Ji, H. C., Lu, H. M., et al. (2019). UPLC-ESI-IT-TOF-MS metabolomic study of the therapeutic effect of Xuefu Zhuyu Decoction on rats with traumatic brain injury. *Journal of Ethnopharmacology, 245*, 112149.

Hsueh, T. P., Sheen, J. M., Pang, J. H., Bi, K. W., Huang, C. C., Wu, H. T., et al. (2016). The anti-atherosclerotic effect of naringin is associated with reduced expressions of cell adhesion molecules and chemokines through NF-κB pathway. *Molecules, 21*(2), 195.

Jiang, H., & Jiang, Y. J. (2016). Effect of serum containing Xuefu Zhuyu Decoction on Expressions of LOX-1, TNF-α, ICAM-1 and VCAM-1 in human vein endothelial cells. *Chinese Journal of Integrative Medicine, 34*(5), 1052–1054.

Jo, J., Leem, J., Lee, J. M., & Park, K. S. (2017). Herbal medicine (Hyeolbuchukeo-tang or Xuefu Zhuyu Decoction) for treating primary dysmenorrhoea: Protocol for a systematic review of randomised controlled trials. *BMJ Open, 7*(6), e015056.

Kamal-Eldin, A., Frank, J., Razdan, A., Tengblad, S., Basu, S., & Vessby, B. (2000). Effects of dietary phenolic compounds on tocopherol, cholesterol, and fatty acids in rats. *Lipids, 35*(4), 427–435.

Kumar, R., Akhtar, F., & Rizvi, S. I. (2020). Hesperidin attenuates altered redox homeostasis in an experimental hyperlipidaemic model of rat. *Clinical and Experimental Pharmacology and Physiology, 47*(4), 571–582.

Li, J., Wang, R. F., Yang, L., & Wang, Z. T. (2015). Structure and biological action on cardiovascularsystems of saponins from *Panax notoginseng. China journal of Chinese materia medica, 40*(17), 3480–3487.

Lin, W. J., Li, S. S., Han, J. D., & Xian, S. Y. (2018). Meta-analysis of supplemented Xuefu Zhuyu Decoction for treating chronic heart failure. *Research and Practice on Chinese Medicines, 32*(6), 65–69.

Lin, Z., Fu, C. C., Yan, Z. J., Wu, Y. F., Zhan, J. D., Lou, Z. L., et al. (2020). The protective effect of hesperetin in osteoarthritis: An *in vitro* and *in vivo* study. *Food & Function, 11*(3), 2654–2666.

Ma, C. R., Xia, R. L., Yang, S., Liu, L. P., Zhang, J., Feng, K., et al. (2020). Formononetin attenuates atherosclerosis via regulating interaction between KLF4 and SRA in apoE mice. *Theranostics, 10*(3), 1090–1106.

Meng, F. S., Lai, H. B., Luo, Z. K., Liu, Y., Huang, X. X., Chen, J. Q., et al. (2018). Effect of Xuefu Zhuyu Decoction pretreatment on myocardium in sepsis rats. *Evidence-based Complementary and Alternative Medicine, 2018*, 2939307.

Qi, J., Cui, J. G., Mi, B. B., Yan, X. H., Xu, W. W., Ma, H., et al. (2020). Isoliquiritigenin inhibits atherosclerosis by blocking TRPC5 channel expression. *Cardiovascular Therapeutics, 2020*, 1926249.

Su, R., Zeng, C., & Zeng, L. (2020). Network pharmacology of Xuefu Zhuyu Decoction in the treatment of endometriosis. *Traditional Chinese Drug Research and Clinical Pharmacology, 31*(3), 330–335.

Sun, L. J., Qiao, W., Xiao, Y. J., Cui, L., Wang, X., & Ren, W. D. (2019). Naringin mitigates myocardial strain and the inflammatory response in sepsis-induced myocardial dysfunction through regulation of PI3K/AKT/NF-κB pathway. *International Immunopharmacology, 75*, 105782.

Tang, F., Yan, H. L., Wang, L. X., Xu, J. F., Peng, C., Ao, H., et al. (2021). Review of natural resources with vasodilation: Traditional medicinal plants, natural products, and their mechanism and clinical efficacy. *Frontiers in Pharmacology, 12*, 627458.

Wang, L. Y., Zhang, Y. P., Mu, Q. X., Yu, H. J., & Wang, Y. F. (2022). Effect of Xuefu Zhuyu Decoction on trimethylamine absorption based on supramolecular sensing technology. *Chinese Traditional and Herbal Drugs, 53*(6), 1783–1789.

Wang, P. Q., Xiong, X. J., & Li, S. J. (2015). Efficacy and safety of a traditional Chinese herbal formula Xuefu Zhuyu Decoction for hypertension: A systematic review and meta-analysis. *Medicine (Baltimore), 94*(42), e1850.

Wang, Q. R. *Yilin Gaicuo* (Qing Dynasty), People's Medical Publishing House, 2005, Beijing.

Wang, S., & Qiu, X. J. (2019). The efficacy of XueFu ZhuYu prescription for hyperlipidemia: A meta-analysis of randomized controlled trials. *Complementary Therapies in Medicine, 43*, 218–226.

Yan, L. J., Wang, S., Zhao, L. L., Qiu, J., Zhou, L., Wang, W. B., et al. (2019). The herb-drug pharmacokinetic interaction of fluoxetine and its metabolite norfluoxetine with a traditional Chinese medicine in rats by LC-MS/MS. *Evidence-based Complementary and Alternative Medicine, 2019*, 2471870.

Yan, S., Wei, P. C., Chen, Q., Chen, X., Wang, S. C., Li, J. R., et al. (2018). Functional and structural characterization of a β-glucosidase involved in saponin metabolism from intestinal bacteria. *Biochemical and Biophysical Research Communications, 496*(4), 1349–1356.

Yang, T., Li, X., Lu, Z., Han, X., & Zhao, M. (2019). Effectiveness and safety of Xuefu Zhuyu Decoction for treating coronary heart disease angina: A systematic review and meta-analysis. *Medicine, 98*(9), 14708.

Yang, J. F., Wang, R., Cheng, X. H., Qu, H. C., Qi, J., Li, D., et al. (2020). The vascular dilatation induced by hydroxysafflor yellow A (HSYA) on rat mesenteric artery through TRPV4-dependent calcium influx in endothelial cells. *Journal of Ethnopharmacology, 256*, 112790.

Zeng, J., Fan, Y. J., Tan, B., Su, H. Z., Li, Y., Zhang, L. L., et al. (2018). Charactering the metabolism of cryptotanshinone by human P450 enzymes and uridine diphosphate glucuronosyltransferases *in vitro*. *Acta Pharmacologica Sinica, 39*(8), 1393–1404.

Zhang, L., Zhu, L., Wang, Y. F., Jiang, Z. Z., Chai, X., Zhu, Y., et al. (2012). Characterization and quantification of major constituents of XueFu ZhuYu by UPLC-DAD-MS/MS. *Journal of Pharmaceutical and Biomedical Analysis, 62*, 203–209.

Zhang, L., Jiang, Z. Z., Yang, J., Li, Y. Y., Wang, Y. F., & Chai, X. (2015). Chemical material basis study of Xuefu Zhuyu Decoction by ultra-performance liquid chromatography coupled with quadrupole time-of-flight mass spectrometry. *Journal of Food and Drug Analysis, 23*(4), 811–820.

Zhang, S., Yuan, M., Cheng, C., Xia, D. H., & Wu, S. W. (2018). Chinese herbal medicine effects on muscle atrophy induced by simulated microgravity. *Aerospace Medicine and Human Performance, 89*(10), 883–888.

Zhang, Y., Kang, A., Deng, H. S., Shi, L., Su, S. L., Yu, L., et al. (2018). Simultaneous determination of sulfur compounds from the sulfur pathway in rat plasm by liquid chromatography tandem mass spectrometry: Application to the study of the effect of ShaoFu ZhuYu Decoction. *Analytical and Bioanalytical Chemistry, 410*(16), 3743–3755.

Zhang, W., Song, J. K., Zhang, X., Zhou, Q. M., He, G. R., Xu, X. N., et al. (2018). Salvianolic acid A attenuates ischemia reperfusion induced rat brain damage by protecting the blood brain barrier through MMP-9 inhibition and anti-inflammation. *Chinese Journal of Natural Medicines, 16*(03), 184–193.

Zhang, Z. D., Yang, Y. J., Liu, X. W., Ma, N., Shen, D. S., & Li, J. Y. (2019). Comparative study of eprinoectin determination in bovine serum samples by three kinds of pre-processimng SPE. *Progress in Veterinary Medicine, 40*, 53–57.

Zhou, Y., Cao, S. J., Wang, Y., Xu, P. X., Yan, J. K., Bin, W., et al. (2014). Berberine metabolites could induce low density lipoprotein receptor up-regulation to exert lipid-lowering effects in human hepatoma cells. *Fitoterapia, 92*(1), 230–237.

Zhu, Y. L., & Zhang, M. (2014). Influence of sodium ferulate injection on levels of blood lipid, nitric oxide and endothelin-1 in patients with coronary heart disease. *Journal of Clinical Medicine in Practice, 18*(23), 11–13.

Zuo, F., Nakamura, N., Akao, T., & Hattori, M. (2006). Pharmacokinetics of berberine and its main metabolites in conventional and pseudo germ-free rats determined by liquid chromatography/ion trap mass spectrometry. *Drug Metabolism and Disposition, 34*(12), 2064–2072.